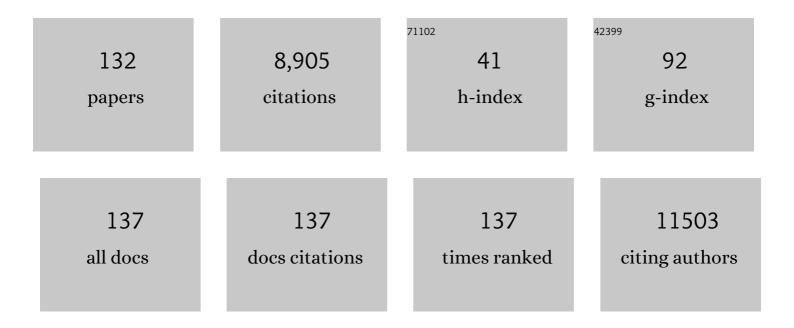
List of Publications by Year in descending order

Source: https://exaly.com/author-pdf/7859524/publications.pdf Version: 2024-02-01



#	Article	IF	CITATIONS
1	Electrochemical Biosensors - Sensor Principles and Architectures. Sensors, 2008, 8, 1400-1458.	3.8	1,607
2	Electrochemical Biosensors - Sensor Principles and Architectures. Sensors, 2008, 8, 1400-1458.	3.8	591
3	Intact Vesicle Adsorption and Supported Biomembrane Formation from Vesicles in Solution:Â Influence of Surface Chemistry, Vesicle Size, Temperature, and Osmotic Pressureâ€. Langmuir, 2003, 19, 1681-1691.	3.5	573
4	Ultrastable Iron Oxide Nanoparticle Colloidal Suspensions Using Dispersants with Catechol-Derived Anchor Groups. Nano Letters, 2009, 9, 4042-4048.	9.1	411
5	Stabilization and functionalization of iron oxide nanoparticles for biomedical applications. Nanoscale, 2011, 3, 2819.	5.6	360
6	Triggered Release from Liposomes through Magnetic Actuation of Iron Oxide Nanoparticle Containing Membranes. Nano Letters, 2011, 11, 1664-1670.	9.1	339
7	Simultaneous Surface Plasmon Resonance and Quartz Crystal Microbalance with Dissipation Monitoring Measurements of Biomolecular Adsorption Events Involving Structural Transformations and Variations in Coupled Water. Analytical Chemistry, 2004, 76, 7211-7220.	6.5	271
8	Vesicle adsorption on SiO2 and TiO2: Dependence on vesicle size. Journal of Chemical Physics, 2002, 117, 7401-7404.	3.0	251
9	A Multitechnique Study of Liposome Adsorption on Au and Lipid Bilayer Formation on SiO2. Langmuir, 2006, 22, 3313-3319.	3.5	224
10	Membrane biosensor platforms using nano- and microporous supports. Trends in Biotechnology, 2008, 26, 82-89.	9.3	206
11	Surface Functionalization of Single Superparamagnetic Iron Oxide Nanoparticles for Targeted Magnetic Resonance Imaging. Small, 2009, 5, 1334-1342.	10.0	203
12	Measuring single-nanoparticle wetting properties by freeze-fracture shadow-casting cryo-scanning electron microscopy. Nature Communications, 2011, 2, 438.	12.8	159
13	Optical Anisotropy of Supported Lipid Structures Probed by Waveguide Spectroscopy and Its Application to Study of Supported Lipid Bilayer Formation Kinetics. Analytical Chemistry, 2008, 80, 3666-3676.	6.5	154
14	Influence of Electronegative Substituents on the Binding Affinity of Catechol-Derived Anchors to Fe ₃ O ₄ Nanoparticles. Journal of Physical Chemistry C, 2011, 115, 683-691.	3.1	142
15	Particle Lithography from Colloidal Self-Assembly at Liquidâ^'Liquid Interfaces. ACS Nano, 2010, 4, 5665-5670.	14.6	141
16	Monodisperse Iron Oxide Nanoparticles by Thermal Decomposition: Elucidating Particle Formation by Second-Resolved in Situ Small-Angle X-ray Scattering. Chemistry of Materials, 2017, 29, 4511-4522.	6.7	102
17	Switching Transport through Nanopores with pH-Responsive Polymer Brushes for Controlled Ion Permeability. ACS Applied Materials & Interfaces, 2013, 5, 1400-1407.	8.0	90
18	Design of Surface Modifications for Nanoscale Sensor Applications. Sensors, 2015, 15, 1635-1675.	3.8	88

#	Article	IF	CITATIONS
19	Nextâ€Generation Polymer Shells for Inorganic Nanoparticles are Highly Compact, Ultraâ€Dense, and Long‣asting Cyclic Brushes. Angewandte Chemie - International Edition, 2017, 56, 4507-4511.	13.8	86
20	Temperature dependence of formation of a supported phospholipid bilayer from vesicles onSiO2. Physical Review E, 2002, 66, 051905.	2.1	82
21	Understanding Ligand Binding Effects on the Conformation of Estrogen Receptor α-DNA Complexes: A Combinational Quartz Crystal Microbalance with Dissipation and Surface Plasmon Resonance Study. Biophysical Journal, 2007, 92, 4415-4423.	0.5	82
22	Adsorption of core-shell nanoparticles at liquid–liquid interfaces. Soft Matter, 2011, 7, 7663.	2.7	78
23	Nanoparticle actuated hollow drug delivery vehicles. Nanomedicine, 2012, 7, 145-164.	3.3	76
24	Formation of supported bacterial lipid membrane mimics. Biointerphases, 2008, 3, FA41-FA50.	1.6	72
25	Synthesis and Magneto-Thermal Actuation of Iron Oxide Core–PNIPAM Shell Nanoparticles. ACS Applied Materials & Interfaces, 2015, 7, 19342-19352.	8.0	65
26	Complete Exchange of the Hydrophobic Dispersant Shell on Monodisperse Superparamagnetic Iron Oxide Nanoparticles. Langmuir, 2015, 31, 9198-9204.	3.5	63
27	Electrically driven nanopillars for THz quantum cascade lasers. Optics Express, 2013, 21, 10917.	3.4	61
28	Rupture Pathway of Phosphatidylcholine Liposomes on Silicon Dioxide. International Journal of Molecular Sciences, 2009, 10, 1683-1696.	4.1	60
29	Analysis of stable self-trapping of laser beams in cubic-quintic nonlinear media. Physics Letters, Section A: General, Atomic and Solid State Physics, 1998, 248, 369-376.	2.1	59
30	Core–shell nanoparticle monolayers at planar liquid–liquid interfaces: effects of polymer architecture on the interface microstructure. Soft Matter, 2013, 9, 3789.	2.7	59
31	Using Complementary Acoustic and Optical Techniques for Quantitative Monitoring of Biomolecular Adsorption at Interfaces. Biosensors, 2012, 2, 341-376.	4.7	56
32	Sequence Controlled Self-Knotting Colloidal Patchy Polymers. Physical Review Letters, 2013, 110, 075501.	7.8	55
33	Individually Stabilized, Superparamagnetic Nanoparticles with Controlled Shell and Size Leading to Exceptional Stealth Properties and High Relaxivities. ACS Applied Materials & Interfaces, 2017, 9, 3343-3353.	8.0	53
34	Core–Shell Structure of Monodisperse Poly(ethylene glycol)-Grafted Iron Oxide Nanoparticles Studied by Small-Angle X-ray Scattering. Chemistry of Materials, 2015, 27, 4763-4771.	6.7	52
35	Poly(methacrylic acid) Grafts Grown from Designer Surfaces: The Effect of Initiator Coverage on Polymerization Kinetics, Morphology, and Properties. Macromolecules, 2009, 42, 1640-1647.	4.8	46
36	Formation of Nanopore-Spanning Lipid Bilayers through Liposome Fusion. Langmuir, 2011, 27, 10920-10928.	3.5	46

#	Article	IF	CITATIONS
37	Single cell 3-D platform to study ligand mobility in cell–cell contact. Lab on A Chip, 2011, 11, 2876.	6.0	45
38	Melt-grafting for the synthesis of core–shell nanoparticles with ultra-high dispersant density. Nanoscale, 2015, 7, 11216-11225.	5.6	45
39	Nanoparticle-triggered release from lipid membrane vesicles. New Biotechnology, 2015, 32, 665-672.	4.4	45
40	Evaluation of High-Yield Purification Methods on Monodisperse PEG-Grafted Iron Oxide Nanoparticles. Langmuir, 2016, 32, 4259-4269.	3.5	45
41	Polymer Topology Determines the Formation of Protein Corona on Core–Shell Nanoparticles. ACS Nano, 2020, 14, 12708-12718.	14.6	45
42	A detailed investigation of the formation kinetics and layer structure of poly(ethylene glycol) tether supported lipid bilayers. Soft Matter, 2009, 5, 2804.	2.7	44
43	Poly(vinyl alcohol) Physical Hydrogels: Noncryogenic Stabilization Allows Nano- and Microscale Materials Design. Langmuir, 2011, 27, 10216-10223.	3.5	43
44	Controlled magnetosomes: Embedding of magnetic nanoparticles into membranes of monodisperse lipid vesicles. Journal of Colloid and Interface Science, 2016, 466, 62-71.	9.4	42
45	From particle self-assembly to functionalized sub-micron protein patterns. Nanotechnology, 2008, 19, 075301.	2.6	41
46	pH- and Electro-Responsive Properties of Poly(acrylic acid) and Poly(acrylic) Tj ETQq0 0 0 rgBT /Overlock 10 Tf 5 Microbalance with Dissipation Monitoring. Langmuir, 2015, 31, 7684-7694.	0 387 Td (3.5	acid)- <i>block 40</i>
47	Simulations of temperature dependence of the formation of a supported lipid bilayer via vesicle adsorption. Colloids and Surfaces B: Biointerfaces, 2004, 39, 77-86.	5.0	39
48	Optimization of Magneto-thermally Controlled Release Kinetics by Tuning of Magnetoliposome Composition and Structure. Scientific Reports, 2017, 7, 7474.	3.3	39
49	Interaction of Size-Tailored PEGylated Iron Oxide Nanoparticles with Lipid Membranes and Cells. ACS Biomaterials Science and Engineering, 2017, 3, 249-259.	5.2	38
50	Controlled aggregation and cell uptake of thermoresponsive polyoxazoline-grafted superparamagnetic iron oxide nanoparticles. Nanoscale, 2017, 9, 2793-2805.	5.6	36
51	Stealth Nanoparticles Grafted with Dense Polymer Brushes Display Adsorption of Serum Protein Investigated by Isothermal Titration Calorimetry. Journal of Physical Chemistry B, 2018, 122, 5820-5834.	2.6	36
52	Mechanical properties of mushroom and brush poly(ethylene glycol)-phospholipid membranes. Soft Matter, 2011, 7, 9267.	2.7	33
53	Surface-active ionic liquids for palladium-catalysed cross coupling in water: effect of ionic liquid concentration on the catalytically active species. RSC Advances, 2017, 7, 41144-41151.	3.6	33
54	Formation of supported lipid bilayers on indium tin oxide for dynamically-patterned membrane-functionalized microelectrode arrays. Lab on A Chip, 2009, 9, 718-725.	6.0	31

#	Article	IF	CITATIONS
55	Lipogels: surface-adherent composite hydrogels assembled from poly(vinyl alcohol) and liposomes. Nanoscale, 2013, 5, 6758.	5.6	31
56	Fabrication of nanoporous silicon nitride and silicon oxide films of controlled size and porosity for combined electrochemical and waveguide measurements. Nanotechnology, 2007, 18, 275303.	2.6	30
57	Advances in nanopatterned and nanostructured supported lipid membranes and their applications. Biotechnology and Genetic Engineering Reviews, 2010, 27, 185-216.	6.2	30
58	Supported Lipopolysaccharide Bilayers. Langmuir, 2012, 28, 12199-12208.	3.5	30
59	Understanding Self-Assembled Amphiphilic Peptide Supramolecular Structures from Primary Structure Helix Propensity. Langmuir, 2008, 24, 7645-7647.	3.5	29
60	Liposomes Tethered to Omega-Functional PEG Brushes and Induced Formation of PEG Brush Supported Planar Lipid Bilayers. Langmuir, 2009, 25, 13534-13539.	3.5	29
61	Simple method for the synthesis of inverse patchy colloids. Journal of Physics Condensed Matter, 2015, 27, 234105.	1.8	29
62	Phospholipase A ₂ -Induced Degradation and Release from Lipid-Containing Polymersomes. Langmuir, 2018, 34, 395-405.	3.5	29
63	Biofilm formation at oil-water interfaces is not a simple function of bacterial hydrophobicity. Colloids and Surfaces B: Biointerfaces, 2020, 194, 111163.	5.0	29
64	Electrochemically Stimulated Release from Liposomes Embedded in a Polyelectrolyte Multilayer. Advanced Functional Materials, 2011, 21, 1666-1672.	14.9	28
65	Design and folding of colloidal patchy polymers. Soft Matter, 2013, 9, 938-944.	2.7	28
66	Whole Genome Sequencing-Based Comparison of Food Isolates of Cronobacter sakazakii. Frontiers in Microbiology, 2019, 10, 1464.	3.5	28
67	Remotely Triggered Liquefaction of Hydrogel Materials. ACS Nano, 2020, 14, 9145-9155.	14.6	28
68	Lipid redistribution in phosphatidylserine-containing vesicles adsorbing on titania. Biointerphases, 2008, 3, FA90-FA95.	1.6	27
69	Quantitative Determination of Dark and Light-Activated Antimicrobial Activity of Poly(Phenylene) Tj ETQq1 1 0.3 Interfaces, 2020, 12, 21322-21329.	784314 rgE 8.0	3T /Overlock 27
70	Triggered Release from Thermoresponsive Polymersomes with Superparamagnetic Membranes. Materials, 2016, 9, 29.	2.9	26
71	Embedded Plasmonic Nanomenhirs as Location-Specific Biosensors. Nano Letters, 2013, 13, 6122-6129.	9.1	25
72	Aggregation of thermoresponsive core-shell nanoparticles: Influence of particle concentration, dispersant molecular weight and grafting. Journal of Colloid and Interface Science, 2017, 500, 321-332.	9.4	24

#	Article	IF	CITATIONS
73	Supported lipid bilayers, tethered lipid vesicles, and vesicle fusion investigated using gravimetric, plasmonic, and microscopy techniques. Biointerphases, 2008, 3, FA108-FA116.	1.6	23
74	Pleckstrin Homology-Phospholipase C-δ1Interaction with Phosphatidylinositol 4,5-Bisphosphate Containing Supported Lipid Bilayers Monitoredin Situwith Dual Polarization Interferometry. Analytical Chemistry, 2011, 83, 6267-6274.	6.5	23
75	Immunogold Nanoparticles for Rapid Plasmonic Detection of C. sakazakii. Sensors, 2018, 18, 2028.	3.8	23
76	Direct C–S bond formation <i>via</i> C–O bond activation of phenols in a crossover Pd/Cu dual-metal catalysis system. Organic and Biomolecular Chemistry, 2019, 17, 4491-4497.	2.8	23
77	Characterization of supported lipid bilayers incorporating and phosphoinositol-3,4,5-triphosphate by complementary techniques. Biointerphases, 2010, 5, 114-119.	1.6	22
78	Design Principles for Thermoresponsive Core–Shell Nanoparticles: Controlling Thermal Transitions by Brush Morphology. Langmuir, 2019, 35, 7092-7104.	3.5	22
79	Nonspecific Colloidal-Type Interaction Explains Size-Dependent Specific Binding of Membrane-Targeted Nanoparticles. ACS Nano, 2016, 10, 9974-9982.	14.6	21
80	Self-Assembly of Iron Oxide-Poly(ethylene glycol) Core–Shell Nanoparticles at Liquid–Liquid Interfaces. Chimia, 2010, 64, 145-149.	0.6	20
81	Magnetoâ€Thermal Release from Nanoscale Unilamellar Hybrid Vesicles. ChemNanoMat, 2016, 2, 1111-1120.	2.8	20
82	Supported lipid bilayer microarrays created by non-contact printing. Lab on A Chip, 2011, 11, 2403.	6.0	19
83	The Role of Chain Molecular Weight and Hofmeister Series Ions in Thermal Aggregation of Poly(2-Isopropyl-2-Oxazoline) Grafted Nanoparticles. Polymers, 2018, 10, 451.	4.5	19
84	Synthesis of short-range ordered aluminosilicates at ambient conditions. Scientific Reports, 2021, 11, 4207.	3.3	17
85	Polymer Brush-Grafted Nanoparticles Preferentially Interact with Opsonins and Albumin. ACS Applied Bio Materials, 2021, 4, 795-806.	4.6	17
86	Characterization of Biofilm Formation by Cronobacter spp. Isolates of Different Food Origin under Model Conditions. Journal of Food Protection, 2019, 82, 65-77.	1.7	16
87	Magnetic Decoupling of Surface Fe ³⁺ in Magnetite Nanoparticles upon Nitrocatecholâ€Anchored Dispersant Binding. Chemistry - A European Journal, 2011, 17, 7396-7398.	3.3	15
88	Real-time analysis of protein and protein mixture interaction with lipid bilayers. Biochimica Et Biophysica Acta - Biomembranes, 2018, 1860, 319-328.	2.6	15
89	Thermoresponsive Core-Shell Nanoparticles: Does Core Size Matter?. Materials, 2018, 11, 1654.	2.9	15
90	Selective (Bio)Functionalization of Solid-State Nanopores. ACS Applied Materials & Interfaces, 2015, 7, 6030-6035.	8.0	14

#	Article	IF	CITATIONS
91	Nextâ€Generation Polymer Shells for Inorganic Nanoparticles are Highly Compact, Ultraâ€Dense, and Longâ€Lasting Cyclic Brushes. Angewandte Chemie, 2017, 129, 4578-4582.	2.0	14
92	Thermoresponsive Polypeptoid oated Superparamagnetic Iron Oxide Nanoparticles by Surfaceâ€Initiated Polymerization. Macromolecular Chemistry and Physics, 2017, 218, 1700116.	2.2	13
93	Influence of Grafted Block Copolymer Structure on Thermoresponsiveness of Superparamagnetic Core–Shell Nanoparticles. Biomacromolecules, 2018, 19, 1435-1444.	5.4	13
94	Affinity Purification and Single-Molecule Analysis of Integral Membrane Proteins from Crude Cell-Membrane Preparations. Nano Letters, 2018, 18, 381-385.	9.1	12
95	Formation and Characteristics of Lipid-Blended Block Copolymer Bilayers on a Solid Support Investigated by Quartz Crystal Microbalance and Atomic Force Microscopy. Langmuir, 2019, 35, 739-749.	3.5	12
96	Thermoresponsive Nanoparticles with Cyclic-Polymer-Grafted Shells Are More Stable than with Linear-Polymer-Grafted Shells: Effect of Polymer Topology, Molecular Weight, and Core Size. Journal of Physical Chemistry B, 2021, 125, 7009-7023.	2.6	12
97	Hybrid lipopolymer vesicle drug delivery and release systems. Journal of Biomedical Research, 2021, 35, 301.	1.6	12
98	Automated time-resolved analysis of bacteria–substrate interactions using functionalized microparticles and flow cytometry. Biomaterials, 2011, 32, 4347-4357.	11.4	11
99	Morpholinium-based ionic liquids show antimicrobial activity against clinical isolates of Pseudomonas aeruginosa. Research in Microbiology, 2021, 172, 103817.	2.1	11
100	DNA Polyelectrolyte Multilayer Coatings Are Antifouling and Promote Mammalian Cell Adhesion. Materials, 2021, 14, 4596.	2.9	11
101	COMPARATIVE PHYSIOCHEMICAL ANALYSIS OF HYDROPHOBINS PRODUCED IN ESCHERICHIA COLI AND PICHIA PASTORIS. Colloids and Surfaces B: Biointerfaces, 2017, 159, 913-923.	5.0	10
102	Nanoparticle Risks and Identification in a World Where Small Things Do Not Survive. NanoEthics, 2017, 11, 283-290.	0.8	10
103	Biocompatible Glyconanoparticles by Grafting Sophorolipid Monolayers on Monodispersed Iron Oxide Nanoparticles. ACS Applied Bio Materials, 2019, 2, 3095-3107.	4.6	10
104	Nanoporous thin films in optical waveguide spectroscopy for chemical analytics. Analytical and Bioanalytical Chemistry, 2020, 412, 3299-3315.	3.7	9
105	Patterning of supported lipid bilayers and proteins using material selective nitrodopamine-mPEG. Biomaterials Science, 2015, 3, 94-102.	5.4	7
106	Previous Homologous and Heterologous Stress Exposure Induces Tolerance Development to Pulsed Light in Listeria monocytogenes. Frontiers in Microbiology, 2016, 7, 490.	3.5	7
107	Cellulosic biofilm formation of Komagataeibacter in kombucha at oil-water interfaces. Biofilm, 2022, 4, 100071.	3.8	7
108	Microarray spotting of nanoparticles. Colloids and Surfaces A: Physicochemical and Engineering Aspects, 2009, 346, 61-65.	4.7	6

#	Article	IF	CITATIONS
109	Host–guest driven ligand replacement on monodisperse inorganic nanoparticles. Nanoscale, 2017, 9, 8925-8929.	5.6	6
110	Fluorescent Magnetopolymersomes: A Theranostic Platform to Track Intracellular Delivery. Materials, 2017, 10, 1303.	2.9	6
111	Poly(ethylene glycol) Grafting of Nanoparticles Prevents Uptake by Cells and Transport Through Cell Barrier Layers Regardless of Shear Flow and Particle Size. ACS Biomaterials Science and Engineering, 2019, 5, 4355-4365.	5.2	6
112	Thermoresponsive Core-Shell Nanoparticles and Their Potential Applications. , 2019, , 145-170.		6
113	Modifying superparamagnetic iron oxide and silica nanoparticles surfaces for efficient (MA)LDIâ€MS analyses of peptides and proteins. Rapid Communications in Mass Spectrometry, 2022, 36, e9212.	1.5	5
114	Nitrocatechol Dispersants to Tailor Superparamagnetic Fe3 O4 Nanoparticles. Chimia, 2010, 64, 826.	0.6	4
115	Preparation and Dynamic Patterning of Supported Lipid Membranes Mimicking Cell Membranes. Methods in Molecular Biology, 2011, 751, 453-463.	0.9	4
116	Minimal Reconstitution of Membranous Web Induced by a Vesicle–Peptide Sol–Gel Transition. Biomacromolecules, 2019, 20, 1709-1718.	5.4	4
117	<i>In Situ</i> Monitoring of Rolling Circle Amplification on a Solid Support by Surface Plasmon Resonance and Optical Waveguide Spectroscopy. ACS Applied Materials & amp; Interfaces, 2021, 13, 32352-32362.	8.0	4
118	NANOSCALE BIOSENSORS AND BIOCHIPS. Annual Review of Nano Research, 2009, , 1-82.	0.2	3
119	Theoretical and Experimental Design of Heavy Metal-Mopping Magnetic Nanoparticles. ACS Applied Materials & Interfaces, 2021, 13, 1386-1397.	8.0	3
120	Nanoparticle interactions with blood proteins and what it means: a tutorial review. Asia-Pacific Journal of Blood Types and Genes, 2019, 3, 73-87.	0.1	3
121	Method for High-Yield Hydrothermal Growth of Silica Shells on Nanoparticles. Materials, 2021, 14, 6646.	2.9	3
122	Cyclodextrin-Appended Superparamagnetic Iron Oxide Nanoparticles as Cholesterol-Mopping Agents. Frontiers in Chemistry, 2021, 9, 795598.	3.6	3
123	Enzymatic Biosensors towards a Multiplexed Electronic Detection System for Early Cancer Diagnostics. , 2007, , .		2
124	Understanding the Photochemical Properties of Polythiophene Polyelectrolyte Soft Aggregates with Sodium Dodecyl Sulfate for Antimicrobial Activity. ACS Applied Materials & Interfaces, 2021, 13, 55953-55965.	8.0	2
125	Investigating retroviral envelope proteome plasticity. Retrovirology, 2013, 10, .	2.0	1
126	Stabilization and Characterization of Iron Oxide Superparamagnetic Core-Shell Nanoparticles for Biomedical Applications. , 2014, , 355-387.		1

#	Article	IF	CITATIONS
127	Crosslinking of floating colloidal monolayers. Monatshefte Für Chemie, 2017, 148, 1539-1546.	1.8	1
128	Effect of deposition angle on fabrication of plasmonic gold nanocones and nanodiscs. Microelectronic Engineering, 2020, 228, 111326.	2.4	1
129	Thermoresponsive block copolymer grafted on core-shell nanoparticles. AIP Conference Proceedings, 2021, , .	0.4	1
130	A microfluidic valve with bubble trap and zero dead volume. Review of Scientific Instruments, 2022, 93, 014105.	1.3	1
131	Editorial commentary on the special issue of Advances in Nanomedicine. Journal of Biomedical Research, 2021, 35, 253.	1.6	Ο
132	Mobile and Three-Dimensional Presentation of Adhesion Proteins Within Microwells. Methods in Molecular Biology, 2013, 1046, 123-132.	0.9	0